Progress In Electromagnetics Research B, Vol. 75, 27–39, 2017

Influences of Damping Resistances on Transient Simulations in Transmission Lines

Afonso J. Prado[1, *], Ketholyn J. Bespalhulk[2], Bruno F. Silva[2], Kassyele O. Conceição[2], Marinez Cargnin-Stieler[2], Elmer M. Gennaro[1], and José Pissolato Filho[3]

Abstract—Simulations of electromagnetic transients in transmission lines can be carried out using simple circuit model. In the case of applications of simple circuit models based on π circuits, there are problems mainly caused by numeric oscillations. The lumped-parameter π equivalent model can be used with some advantages. The numeric integration method applied to the simulations of electromagnetic transients is the trapezoidal rule. If this numeric method is associated with the π equivalent model, results obtained from the simulations are distorted by Gibbs' oscillations or numeric ones. The introduction of damping resistance parallel to the series RL branch of the π equivalent model can mitigate Gibbs' oscillations in obtained results. Voltage peaks caused by these oscillations can also be decreased. So, in this paper, the combined influences of the introduction of damping resistance, the number of π circuits and the time step are investigated searching for minimizing Gibbs' oscillations and the voltage peaks in electromagnetic transient simulations. For this, transient simulations are exhaustively carried out for determining the highest voltage peaks, ranges of damping resistances and other parameters of the model, which minimize these voltage peaks caused by Gibbs' oscillations.

1. INTRODUCTION

Differential linear systems can be applied to describe electromagnetic transient phenomena in transmission lines. Solutions for these systems are obtained using mathematical tools based on the time domain or the frequency one as well as the phase domain or the mode one. Differential equations are numerically solved by integration methods when analytical models are not applicable [1, 2]. In general, the performance and accuracy of numeric methods are related to integration steps (interval between two adjacent points of the numeric calculation) and the tools for determining the initial values of the numeric methods. Among these numerical tools, the methods of Euler, Runge-Kutta, Heun, and Adams can be considered. Euler's method is a variation of the Taylor series where the series are truncated at the first order approximation. It is simple, but it is necessary to apply small integration steps to get good accuracy. Runge-Kutta's method allows rapid changes in integration step, but the computational time should be large to avoid rounding errors. Adams' method is based on simple expressions, but its initial values should be determined by another method. Heun's method, or trapezoidal rule, transforms sets of differential equations into sets of algebraic equations [3]. However, it is prone to sudden changes in values used for its application [4, 5]. Because of the simplicity and better accuracy than Euler's method, the trapezoidal rule is chosen for the application in Electromagnetic Transient Program (EMTP) and Alternative Transient Program (ATP) [6]. The infinitesimal unit model of transmission lines can be represented by a lumped-parameter π equivalent model. Lumped-parameter π equivalent models can be directly applied in phase-domain [1–7]. Generally, domain transformations

Received 27 September 2016, Accepted 22 April 2017, Scheduled 11 May 2017

* Corresponding author: Afonso Jose do Prado (afonsojp@uol.com.br).

[1] São Paulo State University, UNESP, Campus of São João da Boa Vista, Brazil. [2] UNEMAT — University of State of Mato Grosso, Brazil. [3] UNICAMP — University of Campinas, Brazil.

are frequency dependent [8–14]. A large number of units of this π equivalent model are necessary for taking into account the distributed characteristic of the transmission line parameters. When π equivalent circuit models are associated to the trapezoidal rule, spurious numeric oscillations, called Gibbs' oscillations, affect simulations of electromagnetic transient phenomena. Gibbs' oscillations are consequence of numeric integration, and they are not real phenomena. They should be mitigated [12].

In this paper, the performance of an algorithm for simulating transient phenomena in transmission lines is exhaustively checked for minimizing numeric oscillations. Several numeric simulations are used, changing the main parameters that influence the accuracy and efficiency of the applied numeric method of integration. For this, considering π equivalent cascade connections, one of the simplest numeric methods is to introduce damping resistances in parallel to the series elements of each π unit [12]. The influences of the number of π circuits, the time step and the damping resistance on the voltage peaks caused by Gibbs' oscillations are analyzed [7, 12]. Using three-dimensional graphics, the ranges of the mentioned parameters are investigated for mitigation of voltage peaks in numeric simulations of electromagnetic transients. It can lead to simulations of electromagnetic transients in transmission lines with reduced computational times for lumped-parameter π equivalent models. To the best of our knowledge, this exhaustive and systematic investigation of the consequences of application of damping resistances in the structure of π circuits for transient simulations in transmission lines has not been carried out, mainly considering the use of three-dimensional graphics for searching for the best values of the analyzed parameters that minimize numeric oscillations.

The remaining of this paper is organized as follows. Related works are in Section 2. Section 3 is related to the presentation of the equivalent transmission line model. In Section 4, the basic concepts of the algorithm applied to numeric simulations are presented. Two sections are used to present the obtained results. In Section 5, the results without influences of damping resistances are shown, and in Section 6, the results with these influences are shown. The comparing results is provided in Section 7. Finally, our conclusions are presented in Section 8 followed by the acknowledgments and references.

2. RELATED WORKS

Electrical power systems with a long extension or wide-area electrical power systems, mainly the electrical transmission systems and electrical circuits that works with very high frequencies can be modeled as transmission lines [6–8, 16–27]. There are delays between the input signals and output ones because of the great extension or very high frequency. Usually, these input and output signals are voltage and currents. For transmission lines, the relations among transversal voltages (v) and longitudinal currents (i) can be described by Eq. (1). The Z matrix is the longitudinal impedance matrix per unit length, and the Y matrix is the transversal admittance matrix per unit length. v and i are the voltage and current vectors, respectively

$$-\frac{dv}{dx} = Z \cdot i \quad \text{and} \quad -\frac{di}{dx} = Y \cdot v \tag{1}$$

Frequency dependent transmission line models can be developed in phase domain or in mode domain. Associated with these transmission line models, time domain or frequency domain can be used for electromagnetic transient analysis solutions [6–10, 16, 17]. Because of these options, there are several models for transmission line representation applied to electromagnetic transient studies [18–20]. One reason for this is the longitudinal parameter frequency dependence [8–10, 17, 19, 27]. With the aim to improve the frequency dependence representation, several models have been suggested [1–27]. In some cases, phase-mode transformation is applied, considering the problem in mode domain and looking for improvement in frequency dependent parameter representation [8–10, 17, 18]. In exact mathematical development, the phase mode transformation matrices depend on the frequency because the longitudinal impedance (Z) and transversal admittance (Y) line matrices are influenced by frequency [10, 19–27]. If this exact mathematical model is applied to softwares, the result can be a slow digital routines for transmission line analyses. An alternative that can be considered is the use of a single real transformation matrix. It is a way to obtain fast transmission line transient simulations as well as to avoid convolution procedures in this simulation type [8, 9, 17]. Clarke's matrix has presented interesting performances for three-phase transmission lines: exact results for transposed cases and negligible errors for non-transposed ones [18]. Based on Eq. (1), the relations among voltages and currents can be expressed

in mode domain applying the mode transformation (T_V and T_I). These determine the exact Z and Y matrices in mode domain:

$$-\frac{d\left(T_V^{-1}v_{MD}\right)}{dx}=Z\cdot T_I^{-1}i_{MD} \text{ and } -\frac{d\left(T_I^{-1}i_{MD}\right)}{dx}=Y\cdot T_V^{-1}v_{MD} \leftrightarrow Z_{MD}=T_V\cdot Z\cdot T_I^{-1} \text{ and } Y_{MD}=T_I\cdot Y\cdot T_V^{-1} \tag{2}$$

In Eq. (2), T_V and T_I matrices are the eigenvector matrices of Z and Y matrices. In general cases, T_V and T_I transformation matrices are different, have complex elements and depend on the frequency [6, 10, 16, 19–27]. For three-phase systems, the eigenvalue matrix, which is a diagonal one, can be obtained by:

$$\lambda = T_I\cdot Y\cdot Z\cdot T_I^{-1}=T_V\cdot Z\cdot Y\cdot T_V^{-1}=Z_{MD}\cdot Y_{MD}=Y_{MD}\cdot Z_{MD}=\begin{bmatrix}\lambda_\alpha & 0 & 0\\ 0 & \lambda_\beta & 0\\ 0 & 0 & \lambda_0\end{bmatrix} \tag{3}$$

For transposed lines, the exact mode transformation matrices can be changed into constant ones. For three-phase lines, an option is Clarke's matrix [1, 2, 6, 8, 9, 17], and this case is shown in Eq. (4).

$$\lambda\approx\lambda_{AP}=T_{CL}\cdot Y\cdot Z\cdot T_{CL}^{-1}=T_{CL}\cdot Z\cdot Y\cdot T_{CL}^{-1} \quad \text{and} \quad T_{CL}=\begin{bmatrix}-1/\sqrt{3} & 1/\sqrt{2} & 1/\sqrt{3}\\ 2/\sqrt{3} & 0 & 1/\sqrt{3}\\ -1/\sqrt{3} & -1/\sqrt{2} & 1/\sqrt{3}\end{bmatrix} \tag{4}$$

Working with these diagonal matrices from Eq. (3) or (4), λ or λ_{AP}, a three-phase transmission line can be modeled as three independent circuits in the mode domain. Each mode circuit can be treated as a mono-phase transmission line. Like the transmission line, the infinitesimal unit of the mode circuit is represented through a π circuit shown in Fig. 1(a) [3]. Simulations and analyses of electromagnetic transients in power systems or electrical circuits are usually based on the matrix numeric applications. They can be carried out using specific programs, such as the EMTP programs [6, 16] and mathematical ones. These simulations and analyses can also be carried out using language programming for applying numeric routines. Generally, for all these cases, the trapezoidal rule, or Heun's method, is applied to numeric integrations.

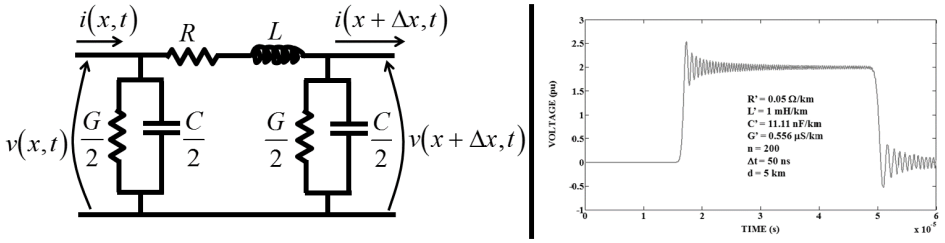

(a) (b)

Figure 1. (a) An infinitesimal unit of a mono-phase transmission line. (b) Voltage step propagation simulation using constant parameters.

Simulating wave propagation for introducing basic concepts of this area to undergraduate students, a simple numeric model has been used, considering constant parameters and frequency dependent ones [1–4]. For simple simulations with constant parameters, a model can be applied based on cascades of π circuits. Considering frequency dependent parameters, cascades is used with modified π circuits [4, 5, 28, 29]. The modified π circuits are obtained from classic π circuits used for simulating introductory cases with frequency independent parameters [29]. Using frequency independent π circuits, the obtained results present undesirable and non-negligible numeric oscillations (Gibbs' oscillations) [1–6, 28, 29]. With modified π circuits, for several analyzed cases, Gibbs' oscillations can be considered negligible.

Based on digital simulations and matrix methods, differential equations and Heun's numeric method for numeric integration, the result of numeric simulation for voltage step propagation through a cascade

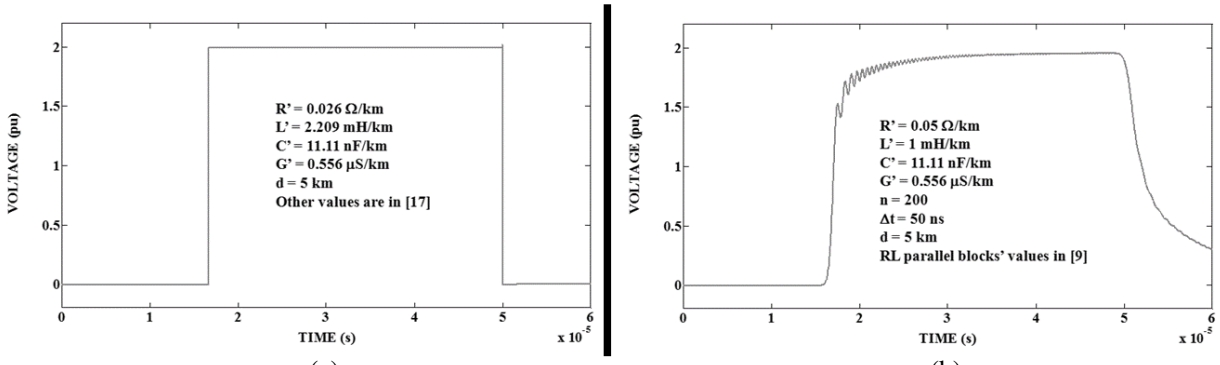

(a) (b)

Figure 2. (a) Voltage step propagation simulation using constant parameters. (b) Result of the application of the numeric Laplace transform.

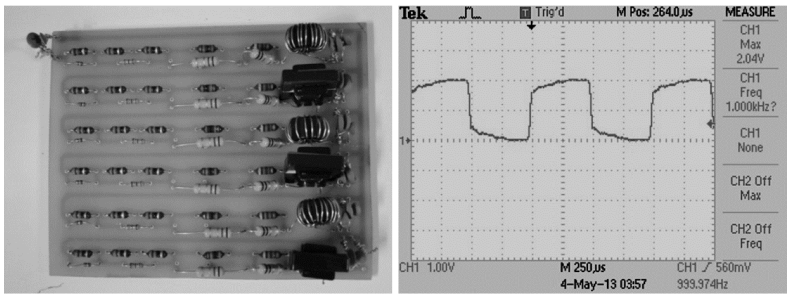

(a) (b)

Figure 3. (a) A module of physical model developed by undergraduate students. (b) Result of voltage step propagation using physical model.

of frequency independent π circuits is shown in Fig. 1(b) [1, 4, 5, 28, 29]. The result obtained using Laplace's numeric method is shown in Fig. 2(a). For introducing the influence of frequency into the simulations with π circuits, the results are shown in Fig. 2(b) [6, 8–10, 18]. Fig. 3(a) shows the module that composes a physical model used to represent the mathematical model with frequency dependent π circuits. In this module, there are six units of modified π circuits. This module has been developed by undergraduate students [30]. The result of voltage step propagation through the physical model is shown in Fig. 3(b). For Figs. 1(b) and 2(b), the parameters are: $R' = 0.05\,\Omega$/km, $L' = 1\,$mH/km, $G' = 0.556\,\mu$S/km and $C' = 11.11\,$nF/km [1, 2, 9]. The length of represented circuit is 5 km. The values of the parameters that introduce the frequency influence are determined by the vector fitting method, and the applied values are previously presented in other papers [11, 29, 31]. For numeric Laplace's transformation and considering the mentioned parameters, the simulation time is 65 µs for a numeric frequency domain technique which is friendly adequate for power system engineers and students [15]. Fig. 2(a) shows only 60 µs of the whole simulation. Analyzing the obtained results, the numeric routine that leads to the results shown in Figs. 1(b) and 2(b) can be changed, avoiding the influence of numeric oscillations. For this, using the introduction of damping resistances is checked, investigating the best ranges for this application [7, 12]. In this case, the models without frequency influence are used. For future, this concept will be introduced in models that consider frequency dependence including comparisons to the physical model shown in Fig. 3(a).

3. EQUIVALENT TRANSMISSION LINE MODEL

From the previous items, differential equations related to numerical simulations of electrical phenomena in transmission lines can be solved by numerical methods decomposing these circuits into infinitesimal

π circuits. The π equivalent cascade connection consists of three different types: the π circuit connected to the sources at the beginning of the line, the π circuit at the end of the line and the intermediate units between the borders of the line [7]. General intermediate circuit cells are represented as shown in Fig. 4(a). Applying Kirchhoff's laws, the differential relations among currents and voltages in Fig. 4(a) are given by Eq. (5). Voltage and current values in the Jth unit depend on the voltage of the previous π circuit and the current of the next π circuit. The mentioned cascade is described by a linear system with $2n$ state variables where n is the number of π circuits in Eq. (6). This linear system is described by Eq. (7). The matrix A, given in Eq. (7), is determined from Eq. (5) [3, 7].

$$\frac{di_J}{dt} = \dot{i}_J = \frac{1}{L}\left(v_{J-1} - R \cdot i_J - v_J\right) \quad \text{and} \quad \frac{dv_J}{dt} = \dot{v}_J = \frac{1}{C}\left(i_J - G \cdot v_J - i_{J+1}\right) \tag{5}$$

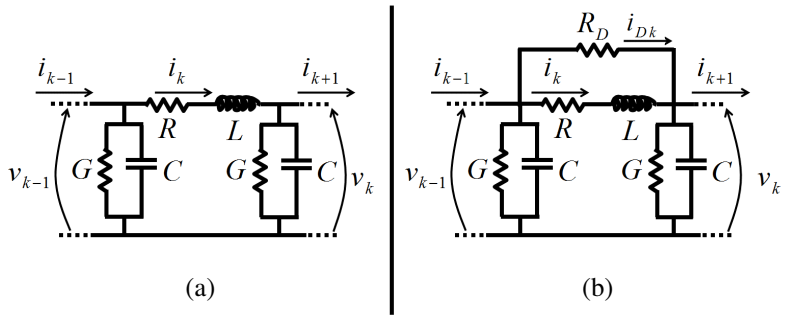

Figure 4. (a) One π equivalent circuit cell for transmission line representation. (b) Modified π equivalent circuit cell with a damping resistance.

$$\dot{x} = Ax + B \quad \text{and} \quad x = \begin{bmatrix} i_1 & v_1 & i_2 & v_2 & i_3 & v_3 & \cdots & i_n & v_n \end{bmatrix}^T \tag{6}$$

$$A = \begin{bmatrix} -R/L & -1/L & 0 & \cdots & \cdots & 0 \\ 1/C & -G/C & -1/C & \ddots & \ddots & \vdots \\ 0 & \ddots & \ddots & \ddots & \ddots & \vdots \\ \vdots & \ddots & 1/C & -G/C & -1/C & 0 \\ \vdots & \ddots & \ddots & 1/L & -R/L & -1/L \\ 0 & \cdots & \cdots & 0 & 2/C & -G/C \end{bmatrix} \tag{7}$$

where:

$$R = R' \cdot \frac{d}{n},\ L = L' \cdot \frac{d}{n},\ G = G' \cdot \frac{d}{n},\ C = C' \cdot \frac{d}{n} \quad \text{and} \quad B = \begin{bmatrix} \frac{1}{L}u_{V1} & \frac{1}{C}u_{I1} & \cdots & \frac{1}{L}u_{Vn} & \frac{1}{C}u_{In} \end{bmatrix}^T \tag{8}$$

Voltage and current sources compose vector B: even lines are related to voltage sources, and odd lines correspond to current sources. Voltage sources are identified by u_{V1}, ..., u_{Vn}, and current ones are identified by u_{I1}, ..., u_{In}. If only one voltage source is connected to the beginning of the line, only u_{V1} element in vector B is non-null [3, 7].

Intermediate π circuits are changed as shown in Fig. 4(b) for introducing damping resistances in parallel to RL series branch [12]. Based on Fig. 4(b), the differential relations are:

$$\dot{i}_J = \frac{v_{J-1} - R \cdot i_J - v_J}{L} \quad \text{and} \quad \dot{v}_J = \frac{i_J - (2G_D + G)\ v_J + G_D\left(v_{J-1} + v_{J+1}\right) - i_{J+1}}{C} \tag{9}$$

Damping resistances and their equivalent conductances are proportional to integer factors (k_D) and inductances of the π circuits (L) and inversely proportional to time steps (Δt) [12]:

$$R_D = k_D \frac{2L}{\Delta t} \quad \leftrightarrow \quad G_D = \frac{1}{R_D} \tag{10}$$

In terms of G_D, changes are made in the elements given by Eq. (11). Other elements of matrix A remain identical to the case without damping resistors.

$$\left.\begin{array}{l} A_{J\,J} = \frac{-(2G_D+G)}{C} \\ A_{J(J-2)} = A_{J(J+2)} = \frac{G_D}{C} \end{array}\right\} \quad J \text{ is even number}, \quad A_{2n\,(2n-2)} = \frac{G_D}{C} \quad \text{and} \quad A_{2n\,2n} = \frac{-\,(2G_D - G)}{C} \tag{11}$$

4. ALGORITHM FOR NUMERIC SIMULATIONS

The trapezoidal rule is a numerical method that transforms differential equations into equivalent algebraic ones. The results of integration are obtained from the area defined by the curve of $f(t)$ at the interval $[t_K,\, t_{K+1}]$ (Fig. 5(a)).

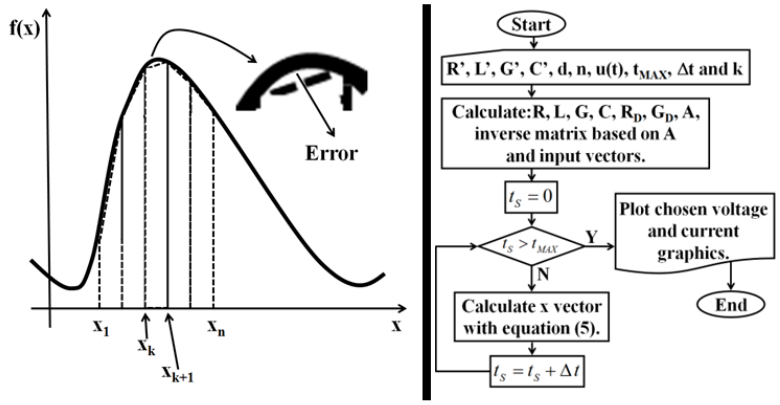

Figure 5. (a) Numeric integration using trapezoidal rule. (b) Flowchart for electromagnetic transient simulations.

The function in the mentioned interval is approximated by the area of a trapezium. Applying the trapezoidal rule, Eq. (12) is obtained, which is related to the time step (Δt).

$$\int_{t(k)}^{t(k+1)} f'(t)\,dt = \frac{\Delta t}{2}\left[f\left(t_{k+1}\right) + f\left(t_k\right)\right] \quad \text{and} \quad \Delta t = t_{k+1} - t_k \tag{12}$$

If point x_K corresponds to $f(t_K)$, and x_{K+1} corresponds to $f(t_{K+1})$, the trapezoidal rule leads to [1–3, 6, 7]:

$$\begin{aligned} x_{K+1} &= x_K + \int_{t(K)}^{t(K+1)} f'(t)\,dt = x_K + \frac{\Delta t}{2}\left[f\left(t_K\right) + f\left(t_{K+1}\right)\right] \quad \rightarrow \\ x_{K+1} &= \left[I - \frac{\Delta t}{2}A\right]^{-1}\left\{\left[I + \frac{\Delta t}{2}A\right]x_K + \frac{\Delta t}{2}\cdot\left(B_{K+1} + B_K\right)\right\} \end{aligned} \tag{13}$$

The flowchart shown in Fig. 5(b) is used for our electromagnetic transient numeric simulations. Line parameters are: $d = 5\,\text{km}$, $T_{MAX} = 150\,\text{ms}$, $C = 11.11\,\text{nF/km}$, $R' = 0.05\,\Omega\text{/km}$, $L' = 1\,\text{mH/km}$, $G' = 0.556\,\mu\text{S/km}$, and the voltage source is a 1 pu voltage step that is connected to the beginning of the line at $t = 0$ [3]. Three parameters are changed, checking for their influences on the voltage peaks at the terminal of the end of the line. The mentioned three parameters are: the number of π circuits, n, the time step, Δt, and the k_D factor. The mentioned influences are caused by combination of damping resistances and the three mentioned parameters. The receiving end terminal is opened, and because of this, and the value of the voltage at this terminal is the double of the value of the voltage at the sending end terminal.

5. RESULTS WITHOUT DAMPING RESISTANCES

Differential analytical relations among voltage and current values in a general π circuit unit are described in Eq. (5). These relations are influenced by electrical variables of the previous π circuit unit and the next one. Correspondent numeric relations present similar dependences, if the A matrix represents the entire π equivalent cascade connection. These dependences are modeled by two non-null sub-diagonals in the A matrix. In this case, the main diagonal of matrix A represents the self-influence of the voltage and current of the unit of the π circuit. In this case, Gibbs' oscillations are not damped during a few time steps after the sudden change on the values of the sources as shown in Figs. 6(a) and 6(b) (1 pu voltage step). Numeric simulations with different time steps are shown in Fig. 6(a). In this case, 200π circuits are used. Changes only in the time steps are not enough to mitigate errors caused by Gibbs' oscillations. With different numbers of π circuits and time step of 50 ns, more numeric simulations are shown in Fig. 6(b). It is also observed that changing only the number of π circuits does not minimize Gibbs' oscillations. For a great number of results, a procedure is developed, which runs several numeric simulations based on the flowchart in Fig. 5(b). In this case, voltage peaks are compared and shown in Fig. 7(a). Based on Fig. 7(a), if a great number of π circuits is applied, values of voltage peaks are about 2.5 pu, corresponding to numeric errors about 25% because the actual value is 2 pu. The lowest values of voltage peaks are related to the minimum number of π circuits, which is 3 units. However, simulations with only 3 units of π circuits lead to results where the electrical waveforms do not reproduce real waveforms propagated during electromagnetic transient phenomena. So, the errors related to voltage peaks decrease, but the waveforms are not sufficiently accurate even for simple analyses (Fig. 7(b)).

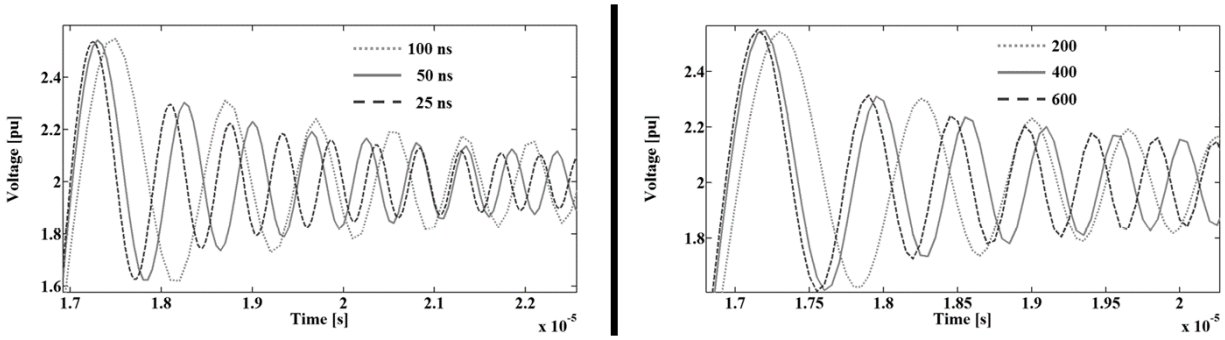

(a) (b)

Figure 6. (a) Simulations for 200 cascaded π circuits without damping resistances. (b) Simulations for 200 cascaded π circuits and 50 ns without damping resistances.

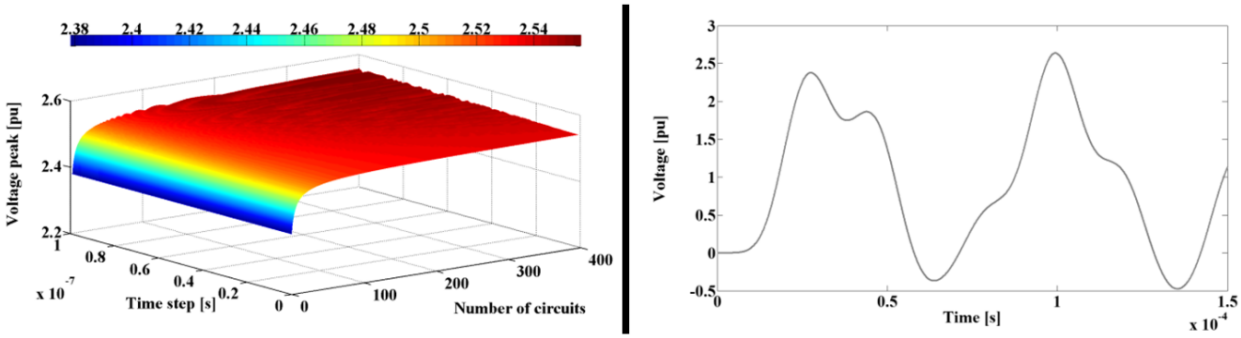

(a) (b)

Figure 7. (a) Voltage peaks of numeric simulations without damping resistances. (b) Numeric simulation of voltage peaks for propagation of voltage step with three π circuits and time step of 50 ns.

Based on Fig. 7(a), it is observed that the combined changes in the time step and number of π circuits cannot mitigate Gibbs' oscillations. In Fig. 7(a), a wide range of time step is used, and the lowest voltage peaks are related to the lowest number of π circuits. As shown in Fig. 7(b), the voltage waveforms are not adequate for electromagnetic transient simulations [1–9]. Fixing the number of π circuits, voltage peaks do not vary significantly as a function of time step as shown Fig. 8(a). Using numbers of π circuits that lead to adequate voltage waveforms for transient simulations, the range of these numbers is applied from 100 to 400. The new three-dimensional graphic is shown in Fig. 8(b). In this case, voltage peaks present variations restricted to a very short interval from 2.52 to 2.56 pu, and these values correspond to about 25% errors because the actual value is 2 pu [7]. Increasing the number of π circuits or decreasing the time step do not influence the errors caused by Gibbs' oscillations.

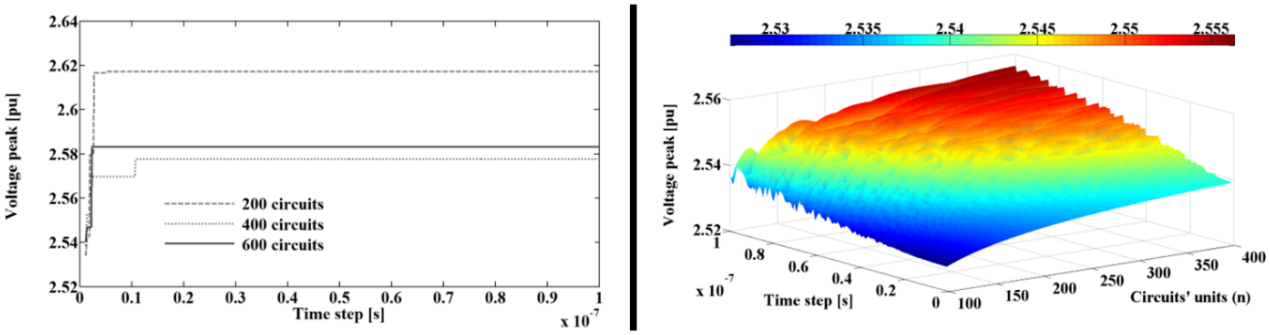

Figure 8. (a) Voltage peaks in function of time step for specific numbers of π circuits. (b) Voltage peaks in function of the time step and the number of π circuits from 100 to 400.

6. RESULTS WITH DAMPING RESISTANCES

Introducing damping resistances in units of π circuits, voltage peaks are decreased depending on the factor k_D. Fig. 9(a) shows simulations that are obtained with three different values of the k_D factor. Fig. 9(b) shows details of Fig. 9(a). When the results of Fig. 7(b) and Fig. 9(a) are compared, it is observed that the simulations without damping resistances and few π circuits lead to a non-useful curve. This curve has voltage peak for the second voltage wave reflection in the receiving end terminal (about 100 ms) higher than the voltage peak for the first voltage wave reflection (about 20 ms).

In the case of Figs. 9(a) and 9(b), the highest voltage peaks occur during the first voltage wave reflection. Considering that the damping resistances are proportional to the inductance and inversely proportional to the time step, changes in these values can influence the damping of Gibbs' oscillations in simulations of electromagnetic transient phenomena. So, Fig. 10 shows a three-dimensional curve that is related to the combined influence of the k_D factor and time step. The inductance is changed when the number of π circuits is changed.

There are other parameters that indirectly influence Gibbs' oscillations. Among these parameters, the number of π circuits can be mentioned. Because the highest voltage peaks occur during the first voltage wave reflection, these values can be used for estimating variations of Gibbs' oscillations. From Fig. 10, voltage peaks are decreased when k_D factor is decreased. Based on Fig. 10, simulations with negligible voltage peaks and influences of Gibbs' oscillations can be obtained as shown in Fig. 11(a). In this case, the parameters mentioned in item III are used. The k_D factor is 3, the time step 100 ns and the number of π circuits 200. It is possible to obtain similar results from Fig. 10 with different combined influences of two variables on voltage peaks among the number of π circuits, time step and factor k_D. Then, Fig. 11(b) shows the combined influence of the π circuits' number and the time step on voltage peaks. In Fig. 12(a), combined influences of factor k_D and number of π circuits on voltage peaks are shown. Fig. 12(b) shows the useful range for numeric electromagnetic transient simulations in which voltage waveforms adequately reproduce the actual phenomena. There are combinations between the factor k_D and number of π circuits that mitigate Gibbs' oscillations.

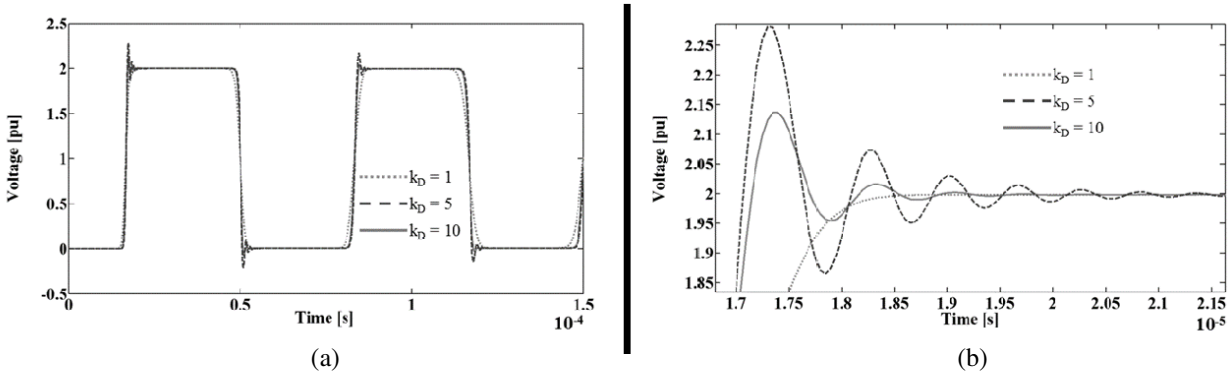

(a) (b)

Figure 9. (a) Simulations with different values of the k_D factor. (b) Details of the first voltage wave reflection observed in Fig. 9.

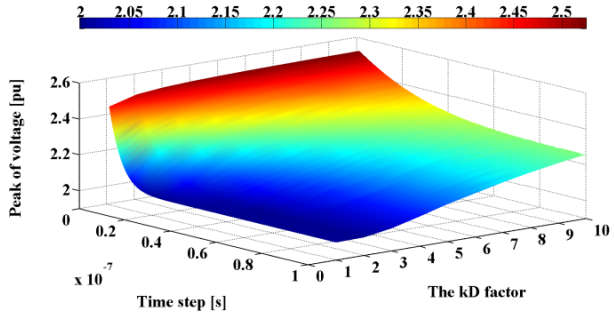

Figure 10. Voltage peaks with damping resistances ($n = 200$) and considering the combined influence of the k_D factor and the time step.

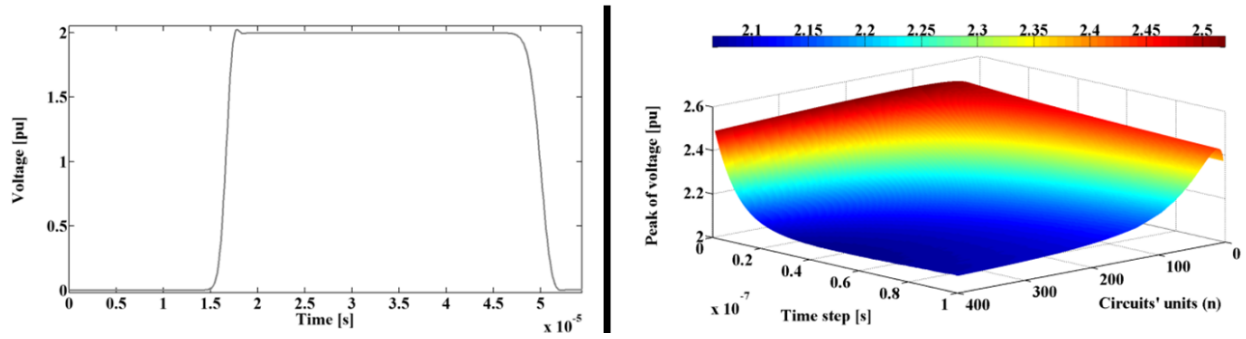

(a) (b)

Figure 11. (a) Simulations with $k_D = 3$ and $\Delta t = 100$ ns for the data mentioned in item III. (b) Voltage peaks with damping resistances ($k_D = 5$) and considering the combined influence of the number of π circuits and the time step.

Using a range of the time step smaller than that considered in Fig. 10, more details are shown in Figs. 13(a) and 13(b). In Fig. 13(a), the range of time step is between 1 ns and 10 ns, and it is between 0.1 ns and 1 ns in Fig. 13(b). If the time step is highly decreased, the voltage peaks are no longer influenced by damping resistances. Based on the results shown in this item, the combined influences of two parameters on the voltage peaks and Gibbs' oscillations are limited for specific ranges. Without the application of damping resistances, voltage peaks are not decreased if the number of π circuits is decreased. Therefore, this is not a useful alternative because the shapes of the curves do not match the

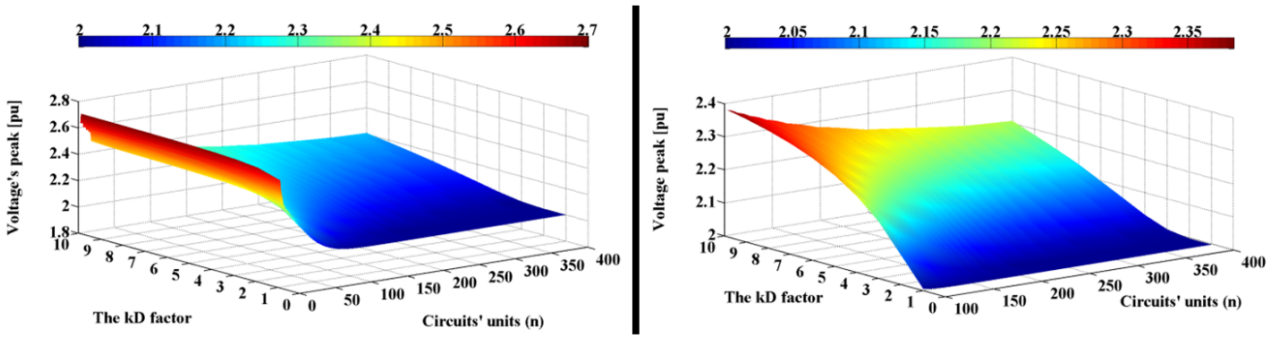

(a) (b)

Figure 12. (a) Voltage peaks with damping resistances ($\Delta t = 50\,\text{ns}$) and influence of the time step and the number of π circuits. (b) The combined influence of the time step and the number of π circuits from 100 to 400.

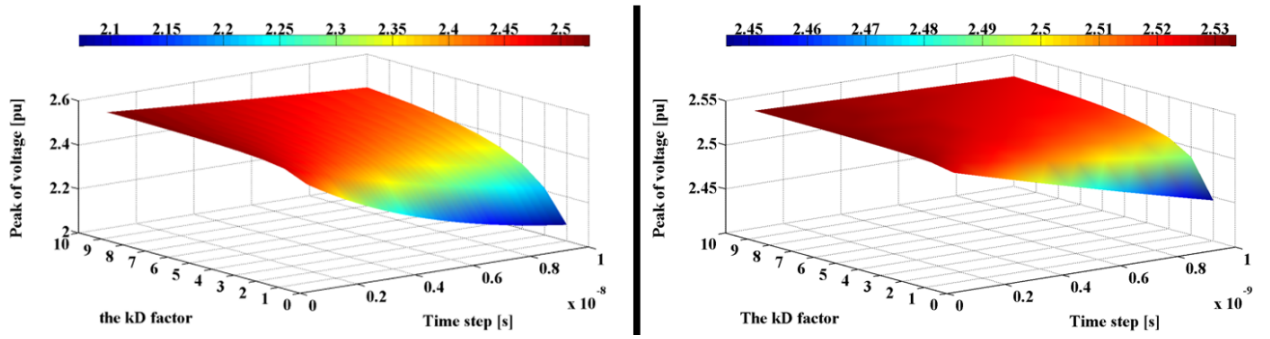

(a) (b)

Figure 13. (a) Details of Fig. 11 for time steps until 10 ns. (b) Details of Fig. 11 for time steps until 1 ns.

actual shapes of the electromagnetic transient phenomena propagated in transmission lines.

Applying damping resistances, besides the k_D factor used for determining R_D in Eq. (10), other line parameters can influence voltage peaks and Gibbs' oscillations, decreasing these numeric errors in numeric simulations. These other line parameters are directly or indirectly related to damping resistances. Damping resistances are inversely proportional to time steps, and because of this, the other mentioned parameters are also related to the time step. In general, one of the main parameters for numeric simulations of electromagnetic transient phenomena is the time step. The introduction of damping resistance is a manner to improve the results of numeric simulations using combined influences of the model's parameters that depend on the time step or the number of π circuits.

7. RESULTS OF COMPARISONS

Based on Fig. 10, simulations with and without the application of damping resistances are compared in Figs. 14(a) and 14(b). In Fig. 14(a), results with the application of damping resistances are compared to correspondent results without the application of damping resistances. In this case, the applied parameters are: time step = 100 ns, $n = 200$ and $k_D = 3$. Most of the parameters used in simulations are shown in Fig. 2. In Fig. 14(a), the specific parameters are time step of 100 ns, $n = 200$ and $k_D = 3$. The specific parameters of Fig. 14(b) are $\Delta t = 60\,\text{ns}$, $n = 300$ and $k_D = 5$, and their determination is based on Fig. 11(b). In Figs. 14(a) and 14(b), results obtained with applications of damping resistances are influenced by Gibbs' oscillations very little. Based on Fig. 9(b), using the k_D factor of 5, the voltage peak error is about 5%. On the other hand, it is not possible to minimize Gibbs' oscillations in simulations carried out without damping resistances. Based on Figs. 7(a), 14(a) and 14(b), without

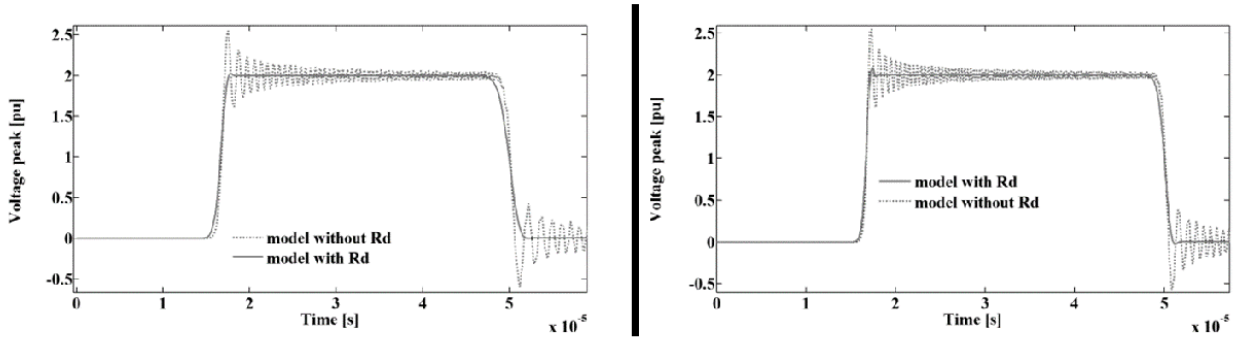

Figure 14. (a) Comparisons of results using $\Delta t = 100\,\text{ns}$, $n = 200$ and $k_D = 3$. (b) Comparisons of results using $\Delta t = 60\,\text{ns}$, $n = 300$ and $k_D = 5$.

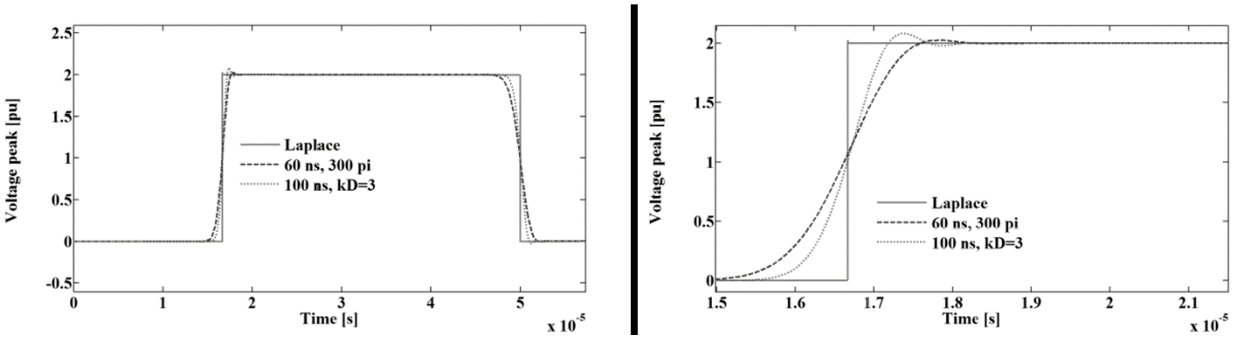

Figure 15. (a) Comparisons considering applications of damping resistances and Laplace's transformation. (b) Details of these comparisons.

damping resistances, voltage peaks errors are always close to 25%.

The results obtained with applications of damping resistances are also compared to results obtained with a numeric routine based on the application of Laplace's transformation [15]. In this case, results of this transformation are considered exact. Fig. 15(a) shows results until the first voltage wave reflection at the sending end terminal of the transmission line.

In Fig. 15(b), details of the first voltage wave reflection at the receiving end terminal are shown. The differences observed between the results of the lumped parameter π equivalent model with damping resistances and the results of numeric solution based on Laplace's transformation are not related to errors caused by Gibbs' oscillations [15]. These differences are related to specific characteristics of considered models and confirm that applications of damping resistances avoid errors caused by Gibbs' oscillations and improve the accuracy of the lumped parameter π equivalent models [7, 15].

8. CONCLUSIONS

Lumped-parameter π equivalent models can be applied to numerically simulating the propagation of electromagnetic transient phenomena in transmission lines. Using the classical structure of this model, these numeric simulations are affected by numeric oscillations or Gibbs' oscillations. It is shown that if damping resistances are included in parallel to RL series branch of the π circuits, Gibbs' oscillations can be mitigated. In the case of this modified structure of π circuits, the highest errors are directly associated with the voltage peaks during the first voltage wave reflection in the receiving end terminal. Damping resistances are proportional to the inductances of π circuits and inversely proportional to the time step. Changes in the time step, the proportional factor for determining damping resistances and the number of π circuits cause proportional changes in Gibbs' oscillations and voltage peaks of propagated

wave. Using these relations, three-dimensional graphics are applied to analyzing combined influences of two parameters on voltage peaks. These three-dimensional graphics can be applied to choosing the best set of the mentioned parameters for obtaining numeric simulations with limited influences of Gibbs' oscillations. Or they can be applied to choosing the set with the minimum number of π circuits and the maximum time step for limited errors caused by Gibbs' oscillations. This can lead to simulations with minimum numerical errors and maximum computational times for lumped-parameter π equivalent models applied to simulations of electromagnetic transients in transmission lines.

ACKNOWLEDGMENT

The authors acknowledge the suggestions to this text of Dr. Marcelo L. F. Abbade, professor at UNESP – Brazil. This work was supported by FAPESP (São Paulo Research Foundation) by process #2015/21390-7.

REFERENCES

1. Macías, J. A. R., A. G. Expósito, and A. B. Soler, "A comparison of techniques for state-space transient analysis of transmission lines," *IEEE Trans. on Power Delivery*, Vol. 20, No. 2, 894–903, April 2005.
2. Macías, J. A. R., A. G. Expósito, and A. B. Soler, Correction to "A comparison of techniques for state-space transient analysis of transmission lines," *IEEE Trans. on Power Delivery*, Vol. 20, No. 3, 2358, July 2005.
3. Nelms, R. M., G. B. Sheble, S. R. Newton, and L. L. Grigsby, "Using a personal computer to teach power system transients," *IEEE Trans. on Power Systems*, Vol. 4, No. 3, 1293–1294, August 1989.
4. Mamis, M. S., "Computation of electromagnetic transients on transmission lines with nonlinear components," *IEE Proc. Generation, Transmission and Distribution*, Vol. 150, No. 2, 200–204, March 2003.
5. Mamis¸, M. S. and M. Koksal, "Solution of eigenproblems for state-space transient analysis of transmission lines," *Electric Power Systems Research*, Vol. 55, No. 1, 7–14, July 2000.
6. Dommel, H. W., *Electromagnetic Transients Program — Rule Book*, Oregon, 1984.
7. Prado, A. J., L. S. Lessa, R. C. Monzani, L. F. Bovolato, and J. Pissolato Filho, "Modified routine for decreasing numeric oscillations at associations of lumped elements," *Electric Power Systems Research*, Vol. 112, No. 1, 56–64, July 2014.
8. Brandão Faria, J. A. and J. Briceño Mendez, "Modal analysis of untransposed bilateral three-phase lines — a perturbation approach," *IEEE Trans. on Power Delivery*, Vol. 12, No. 1, January 1997.
9. Brandão Faria, J. A. and J. Briceño Mendez, "On the modal analysis of asymmetrical three-phase transmission lines using standard transformation matrices," *IEEE Trans. on Power Delivery*, Vol. 12, No. 4, October 1997
10. Morched, A., B. Gustavsen, and M. Tartibi, "A universal model for accurate calculation of electromagnetic transients on overhead lines and underground cables," *IEEE Trans. on Power Delivery*, Vol. 14, No. 3, 1032–1038, July 1999.
11. Gustavsen, B. and A. Semlyen, "Combined phase and modal domain calculation of transmission line transients based on vector fitting," *IEEE Trans. on Power Delivery*, Vol. 13, No. 2, April 1998.
12. Chrysochos, I., G. P.Tsolaridis, T. A. Papadopoulos, and G. K. Papagiannis, "Damping of oscillations related to lumped-parameter transmission line modeling," *Conf. on Power Systems Transients (IPST 2015)*, 7, 2015.
13. Galvão, R. K. H., S. Hadjiloucas, K. H. Kienitz, H. M. Paiva, and R. J. M. Afonso, "Fractional order modeling of large three-dimensional RC networks," *IEEE Trans. Circuits and Systems – I: Regular Papers*, Vol. 60, No. 3, 624–637, March 2013.
14. Gustavsen, B., "Avoiding numerical instabilities in the universal line model by a two-segment interpolation scheme," *IEEE Trans. Power Delivery*, Vol. 28, No. 3, July 2013.

15. Moreno, P. and A. Ramirez, "Implementation of the numerical Laplace transform: A review," *IEEE Trans. on Power Delivery*, Vol. 23, No. 4, October 2008.
16. *Microtran Power System Analysis Corporation, Transients Analysis Program Reference Manual*, Vancouver, Canada, 1992.
17. Brandão Faria, J. A., "Overhead Three-phase Transmission Lines – Non-diagonalizable situations," *IEEE Transactions on Power Delivery*, Vol. 3, No. 4, October 1988.
18. Clarke, E., *Circuit Analysis of AC Power Systems*, Vol. I, Wiley, New York, 1950
19. Wedepohl, L. M., H. V. Nguyen, and G. D. Irwin, "Frequency-dependent transformation matrices for untransposed transmission lines using Newton-Raphson method," *IEEE Trans. on Power Systems*, Vol. 11, No. 3, 1538–1546, August 1996.
20. Nguyen, T. T. and H. Y. Chan, "Evaluation of modal transformation matrices for overhead transmission lines and underground cables by optimization method," *IEEE Trans. on Power Delivery*, Vol. 17, No. 1, January 2002.
21. Nobre, M., W. C. Boaventura, and W. L. A. Neves, "Phase-domain network equivalents for electromagnetic transient studies," *The 2005 IEEE Power Engineering Society General Meeting*, CD-ROM, San Francisco, USA, June 12–16, 2005.
22. Budner, A., "Introduction of frequency dependent transmission line parameters into an electromagnetic transients program," *IEEE Trans. on Power Apparatus and Systems*, Vol. 89, 88–97, January 1970.
23. Carneiro, Jr., S., J. R. Martí, H. W. Dommel, and H. M. Barros, "An efficient procedure for the implementation of corona models in electromagnetic transients programs," *IEEE Transactions on Power Delivery*, Vol. 9, No. 2, April 1994.
24. Martins, T. F. R. D., A. C. S. Lima, and S. Carneiro, Jr., "Effect of impedance approximate formulae on frequency dependence realization," *The 2005 IEEE Power Engineering Society General Meeting*, CD-ROM, San Francisco, USA, June 12–16, 2005.
25. Marti, J. R., "Accurate modelling of frequency-dependent transmission lines in electromagnetic transients simulations," *IEEE Trans. on PAS*, Vol. 101, 147–155, January 1982.
26. Wedepohl, L. M., "Application of matrix methods to the solution of travelling-wave phenomena in polyphase systems," *Proceedings IEE*, Vol. 110, 2200–2212, December 1963.
27. Wedepohl, L. M. and D. J. Wilcox, "Transient analysis of underground power-transmission system — system model and wave propagation characteristics," *Proceedings of IEE*, Vol. 120, No. 2, 253–260, 1973.
28. Mamis¸ M. S. and M. E. Meral, "State-space modeling and analysis of fault arcs," *Electric Power Systems Research*, Vol. 76, Nos. 1–3, 46–51, September 2005.
29. Prado, A. J., S. Kurokawa, J. Pissolato Filho, L. F. Bovolato, and E. C. M. Costa, *Phase-mode Transformation Matrix Application for Transmission Line and Electromagnetic Transient Analyses*, Nova Science Publisher, Inc., Hauppauge, NY, 2011.
30. Andrade, P. R., R. C. Monzani, L. S. Lessa, T. Ingelbinck, A. J. Prado, J. Pissolato Filho, and L. F. Bovolato, "Physical model for representing transmission lines by undergraduate students," *The 10th Latin-American Congress on Electricity Generation and Transmission — CLAGTEE 2013*, CD-ROM, 5, Viña del Mar, Chile, 6–9 de outubro de 2013.
31. Gustavsen, B. and A. Semlyen, "Rational approximation of frequency domain responses by vector fitting," *IEEE Trans. on Power Delivery*, Vol. 14, No. 3, July 1999.